Application of SMR to modeling watersheds in the Catskill Mountains

Vishal K. Mehta [a], M. Todd Walter [a,*], Erin S. Brooks [b], Tammo S. Steenhuis [a], Michael F. Walter [a], Mark Johnson [a], Jan Boll [b] and Dominique Thongs [c]

[a] *Department of Biological and Environmental Engineering, Cornell University, Ithaca, NY 14853-5701, USA*
E-mail: mtw5@cornell.edu
[b] *Department of Biological and Agricultural Engineering, Moscow, ID 83844, Russia*
[c] *New York City Dept. of Environmental Protection, Kingston, NY 12401, USA*

Very few hydrological models commonly used in watershed management are appropriate for simulating the saturation excess runoff. The Soil Moisture Routing model (SMR) was developed specifically to predict saturation excess runoff from variable source areas, especially for areas where shallow interflow controls saturation. A recent version of SMR was applied to two rural catchments in the Catskill Mountains to evaluate its ability to simulate the hydrology of these systems. Only readily available meteorological, topographical, and landuse information from published literature and governmental agencies was used. Measured and predicted streamflows showed relatively good agreement; the average Nash–Sutcliffe efficiency for the two watersheds were $R^2 = 72\%$ and $R^2 = 63\%$. Distributed soil moisture contents and the locations of hydrologically sensitive areas were also predicted well.

Keywords: Soil Moisture Routing model, distributed watershed modeling, saturation excess runoff, variable source area hydrology, distributed soil moisture, NYC watersheds

1. Introduction

In humid, temperate climates runoff is commonly generated from areas in the landscape where the soil has saturated to the surface (e.g., [1]). This process is commonly referred to as *saturation excess* runoff. A counterpart runoff process is *infiltration excess* runoff, which occurs when the rainfall intensity exceeds the land's infiltration capacity (e.g., [2,3]). Because humid, well-vegetated areas, such as the Catskill Mountains of New York State, commonly have higher soil infiltration capacities than rainfall intensities, infiltration excess is rare and saturation excess is the dominant runoff process [4]. Due to drainage and evapotranspiration, the location and extent of saturated runoff-generating areas are dynamic. The term *variable source area* (VSA) hydrology refers to this type of system [1].

There are very few models that are designed to simulate VSA hydrology, and fewer yet that have modest enough data-input requirements to be readily used by watershed planners and managers. Most commonly used models represent relatively large portions of watersheds as lumped hydrological units and, therefore, cannot be used to identify discrete, saturated areas in the landscape, e.g., AGNPS [5], SWAT, SWRRB [6]. Many of these models also base the runoff potential of each portion of the landscape on landuse and soil infiltration capacity and, thus, these models are implicitly most applicable to infiltration excess dominated systems. Of the few distributed models that simulate VSA hydrology, most require large amounts of input data, much of which is typically unavailable, making these models untenable to watershed managers, planners, and other practitioners (e.g., [7–9]).

The Soil Moisture Routing model (SMR) was developed primarily for practitioners to simulate VSA hydrology in shallow-soil interflow driven systems [10]. Specifically, SMR is a management tool used to locate runoff-contributing areas that vary spatially and temporally with the rise and fall of shallow, transient, perched groundwater. One impetus for developing SMR was the need for a hydrological model that could be used to develop land management practices in the New York City (NYC) watersheds for water quality [11]. SMR is especially well suited to the NYC watersheds in the Catskill Mountains, which are characterized by hilly topography with shallow, permeable soils overlaying restrictive bedrock or fragipans [10]. Accurately estimating the locations of runoff source areas in the landscape is important to developing effective management practices [12]. For management purposes, SMR is used to identify Hydrologically Sensitive Areas (HSA), which are areas prone to being runoff source areas, and typically form where shallow, perched groundwater accumulates and saturates the soil profile. Knowing the spatio-temporal distribution of HSA's allows watershed planners to develop management strategies that avoid placing potential pollutants on these HSA's.

Prior to developing SMR, hydrologists working in the NYC watersheds considered TOPMODEL [13,14] as a possible hydrological model to use in the Catskills because it was a popular semi-distributed hydrological model that simulates VSA hydrology [15]. However, it was discarded because its conceptual basis was not well-suited for shallow systems, driven by transient interflow [10,16,17].

* Corresponding author.

The objective of this project was to test SMR under conditions typical to most management scenarios, specifically applying the model to medium-sized watersheds, 10–50 km², using only open-access data for inputs. SMR has been shown to work well under research settings utilizing small, easily parameterized watersheds for which on-site soil characteristics and meteorological data were collected specifically for model testing [10,18]. In essence, these tests demonstrated the adequacy of SMR's conceptual and mathematical bases. Hydrological models are commonly tested using experimental, research watersheds with substantial monitoring and instrumentation to collect field data that are used to corroborate and calibrate models. In management situations, this is an exception rather than the norm, and the need to apply modeling tools to typical situations using only readily available data should be recognized. Further, because models with significantly different structures can perform comparably well in simulating some particular output, most commonly, streamflow [19], it is insufficient to only show that the model can correctly simulate streamflow hydrographs. Therefore, this study tested SMR's ability to correctly simulate processes internal to a watershed by corroborating simulated soil moisture and saturated areas against field measurements. It was also important to test the model's reliability for correctly locating saturated areas because, as discussed earlier, reliable estimates of HSA's is critical to watershed management plans for water quality.

2. SMR overview

The inspiration for SMR's [10] conceptual basis was a hydrologic model for shallow soils [20] that incorporated a philosophy that model complexity should be balanced with input-data precision and hydrological-complexity. SMR is a hydrological modeling concept with a growing set of tools for addressing particular sub-processes as needed such as snowmelt, surface flow routing, and macropore flow. Several researchers have contributed to the model's development and its current, fully distributed form [15,18,21–24]. Presented here is a brief description of a recent version of SMR with emphasis on changes from the original model [10,25]. One notable change from the early versions of SMR is that the shallow soil is modeled as a series of layers rather than a single layer to allow more realistic moisture distribution throughout the soil profile [18,23].

SMR is based on a water balance performed on each grid cell of the watershed (figure 1). For each soil layer of each cell, the water balance is calculated at each time step 'dt' as,

$$D_i \frac{\mathrm{d}\theta_i}{\mathrm{d}t} = P - ET_i + \frac{\sum Q_{\text{in}} - \sum Q_{\text{out}}}{A} - L_i - R_i, \quad (1)$$

where i is the cell address, D is the soil depth of the cell [L], θ is the volumetric moisture content of the cell [L³L⁻³], P is rain plus snowmelt [LT⁻¹], ET is the actual evapotranspiration [LT⁻¹], $\sum Q_{\text{in}}$ is the lateral inflow from surrounding upslope cells [L³T⁻¹], $\sum Q_{\text{out}}$ is the lateral outflow to surrounding downslope cells [L³T⁻¹], L is the leakage from one layer to the layer below [LT⁻¹], R is surface runoff [LT⁻¹], A is the area of a cell [L²]. Note that for all but the surface layer, P is actually leakage from the layer above. For the bottom layer, L is the deep percolation out of the soil profile into the bedrock reservoir. Figure 1 illustrates the components of the water balance for a two-layered soil. The water balance is most commonly performed on a daily time step and the number of soil layers used depends on data availability. Component processes are presented below in the order that they are calculated in the model at each time step, for every grid cell in the watershed. The step-wise calculation approach keeps simulation time short.
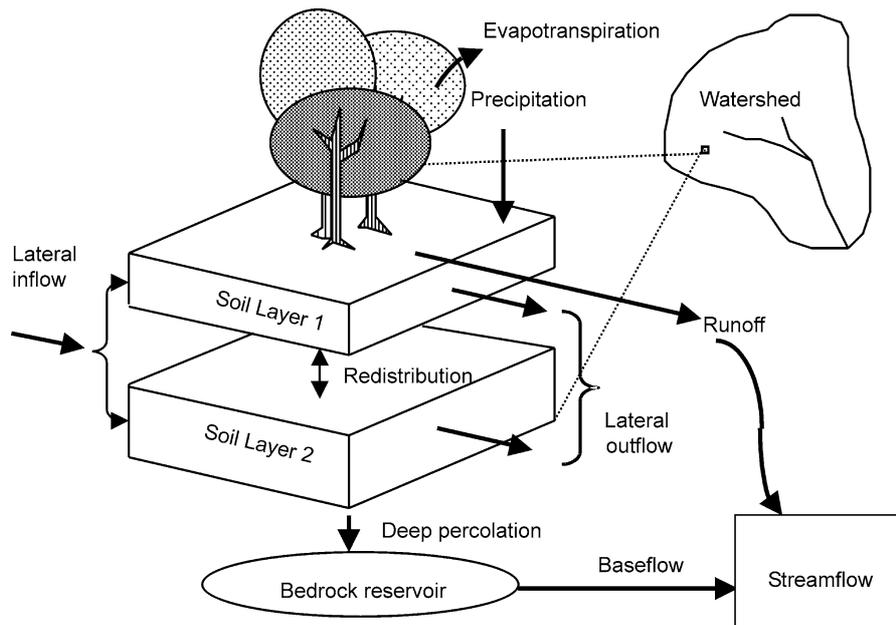

Figure 1. Conceptual schematic of SMR.

2.1. Precipitation and infiltration

Precipitation inputs include rainfall and snowmelt. Precipitation when the mean daily temperature is below 0°C falls as snow. Snowmelt is estimated using a temperature index method [26] and air temperature is distributed throughout the watershed using the dry adiabatic lapse rate [23]. Since saturated hydraulic conductivities and, thus, soil infiltration capacities, are generally higher than rainfall intensities [4], all precipitation infiltrates into the soil. Soil moisture is then redistributed among the layers proportional to the available water storage capacity of each layer. If the storage capacity for all layers in a cell is satisfied, the soil profile starts saturating from the bottom [10].

2.2. Subsurface lateral flow

Subsurface lateral flow, or interflow, leaving each cell is calculated from Darcy's law using the kinematic approximation, i.e., the hydraulic gradient is approximated by the land slope of each cell. The effective lateral hydraulic conductivity, $K(\theta)$, for the vadose zone is simulated as a dual permeability model [27], with distinct equations applied to two flow regimes, one dominated by matrix flow and the other by preferential flow through macropores. The two flow regimes are differentiated by a critical or boundary moisture content, θ_B, above which subsurface flow is dominated by macropore flow and below which subsurface flow is dominated by matrix flow. For each layer j of cell i,

$$K(\theta) = K_s \exp\left(-\alpha \frac{\theta_s - \theta}{\theta_s - \theta_B}\right) \quad \text{for } \theta < \theta_B, \quad (2)$$

$$K(\theta) = \left[m K_s - K(\theta_B)\right]\left(\frac{\theta - \theta_B}{\theta_s - \theta_B}\right) + K(\theta_B)$$
$$\text{for } \theta_s \geqslant \theta > \theta_B, \quad (3)$$

where K_s is the saturated conductivity [LT^{-1}], θ_s is the saturated moisture content [L^{3}L^{-3}], α is a constant, found to be equal to 13 [28,29], and m is the macroporosity factor for each layer [23]. Accounting for macroporosity is consistent with observations that Soil Survey permeabilities are commonly lower than field measured K_s because Soil Survey procedures often do not incorporate macropore flow [30]. One to two orders of magnitude differences between field measured K_s and Soil Survey permeabilities are common [15,23,31,32]. The macroporosity factor, m, decreases with depth reflecting decreasing macroporosity with depth [33,34].

Subsurface lateral flow is divided among all downhill neighbors using a multiple flow path algorithm. This water is added to cells at the beginning of the next time step.

2.3. Evapotranspiration (ET)

ET calculations are the same as in the originally published model [10].

2.4. Deep percolation

In SMR, if the soil profile is above field capacity, water drains at a rate controlled by the restricting subsurface (bedrock or fragipan) into a lumped 'groundwater reservoir'. Below field capacity there is no drainage. Recharge into this conceptual reservoir is determined by the effective subsurface conductivities of the bedrock or fragipan (L in (1)). Unfortunately, there is very little information available regarding percolation rates through these materials. This study used an effective fragipan conductivity of 0.01 cm d^{-1} [23] and effective bedrock conductivity of 0.18 cm d^{-1}. These fragipan and bedrock conductivities are within the range mentioned in [15,35]. A map of the restricting layer was created from drainage information and parent material data available in Soil Surveys.

2.5. Runoff

As in the originial SMR [10], surface runoff is generated by summing excess moisture above saturation for all surface cells.

2.6. Baseflow

Baseflow is only of concern for simulating streamflow hydrographs, i.e., it does not affect the simulation of saturated areas or runoff. Baseflow is simulated using a simple linear reservoir model to drain the lumped groundwater reservoir. Based on extensive recession flow analyses for the Catskills region of New York, the linear reservoir coefficient used is 0.1 d^{-1} [36].

2.7. Streamflow

Streamflow is simulated by summing runoff, baseflow, and interflow from cells adjacent to stream channels.

3. Site description

The model was tested on two rural watersheds, Town Brook (37 km^2) and Biscuit Brook (9.6 km^2), in the Catskill Mountains of New York State (NYS), within the NYC watershed (figure 2). The Hudson River Valley distinctly bounds the Catskills on the east. From the eastern Catskills escarpment, the mountains grade west into the Alleghany Plateau, which stretches across the southern tier of NYS. Glacial till, the parent material for most soils in the region, is thin on the ridges and upper slopes where soils overlay fractured bedrock while it is up to several meters thick in the lower slopes where the soils typically overlay a dense fragipan [37]. The region is hydrologically characterized by steep slopes and shallow permeable soils over a restrictive layer. The climate is characteristically humid, with an average annual temperature of 8°C and an average annual precipitation of 1123 mm.
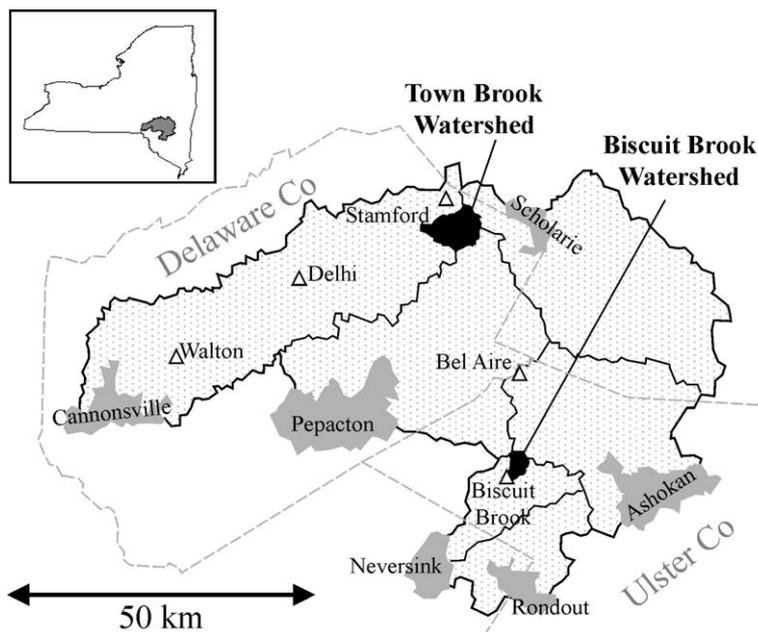
Figure 2. West of Hudson watersheds showing the Town Brook and Biscuit Brook watersheds and weather stations (inset: NYS map and study area).

Town Brook drains into the West Branch of the Delaware River and the elevation ranges from 493 to 989 m and the slopes are as steep as 43°. The watershed is a sub-catchment of the Cannonsville basin and 50% of the area is forested, 20% is rotated in corn and hay, and the remaining area is mostly scrub-land and permanent pasture. Dairy farming is the main agricultural landuse in the watershed. Almost 60% of the watershed is underlain by a restrictive fragipan, the rest is underlain by fractured bedrock [37]. Elevations in the Biscuit Brook watershed ranges from 627 to 1129 m and hillslopes are as steep as 46°. The watershed is entirely forested and drains directly into the West Branch of the Neversink River. The entire watershed is underlain by fractured bedrock [37].

4. Input data

4.1. Weather data

Daily precipitation and daily average temperature are the primary weather inputs for SMR.

Town Brook. Town Brook demonstrated a common problem with these types of data, namely incomplete records for the closest sources. Therefore, input data were composed of the most local data when available and supplemented with more distantly collected data as needed. The Town Brook simulations spanned a period from 4/1/97 to 4/30/01. USGS temperature data from within Town Brook were available from 9/22/98–4/30/01. The nearest temperature data for the rest of the simulation period were from the National Climate Data Center (NCDC) located at Delhi, NY (42°15′N, 74°54′W, elevation 438.9 m) (figure 2). Precipitation data collected inside the watershed by the USGS were

available from 7/26/00–4/30/01. For those periods when within-watershed data were unavailable, precipitation data from the NCDC at Stamford, located just north of the watershed (42°22′N, 74°39′W, elevation 542.2 m), were used (figure 2).

Biscuit Brook. Biscuit Brook was modeled for 1999 and precipitation data were available from within the watershed from the USGS meteorological station (ID NY68), part of the National Atmospheric Deposition Project (NADP). Temperature data from the NYC-DEC's meteorological station at Bel Aire Mountain (ID 556503) approximately 20 km away were used (figure 2).

4.2. Input maps and interpretation

SMR requires three, primary input maps: elevation, soils and landuse. These three digital maps were used similarly for both watersheds.

Digital Elevation Model (DEM). The 7.5 min, 10 m resolution, USGS Digital Elevation Models (DEM) were downloaded from the Cornell University Geospatial Information Repository (CUGIR) website for the respective quads in Delaware and Ulster Counties, encompassing the Town Brook and Biscuit Brook watersheds, respectively (http://gis.mannlib.cornell.edu). A 10 m resolution generally captures topography effectively enough for SMR [24].

Landuse. Digital landuse maps for the Town Brook and Biscuit Brook watersheds were obtained from the NYC-DEP. The 10 m × 10 m grid represents a Landuse Analysis, in which the original 25 m grid coverage was enhanced with information regarding roads and developed areas (NYC-DEP, personal correspondence, 2000). The original 25 m

grid was, in turn, developed from two LANDSAT Thematic Mapper (TM) scenes from July 25, 1992 and May 9, 1993. The landuse categories were reclassified to five types – forest, grass, corn, impervious areas and water bodies – and monthly ET coefficients were assigned to each [23].

Soils. Digital soil maps for Town Brook were obtained from the Soil Survey Geographic (SSURGO) data along with associated attribute tables (Map Unit Identification Records (MUIR)), which were used to extract soil properties. For Biscuit Brook, SSURGO data were unavailable so a digital soil map, obtained from the NYC-DEP, was utilized and soil attributes were obtained from [38].

Five soil properties – soil depth, porosity, field capacity, wilting point, K_s – are required input data for each layer of each soil type. For Town Brook, depth, bulk density, permeability, and percentage rock fragments were obtained from MUIR. The original Soil Survey [38] was used for extracting the same soil properties for Biscuit Brook. In cases where a range of values was given, a simple arithmetic mean was assigned. Porosity was derived from bulk density and permeability was used to approximate K_s. Percentage rock fragments were subtracted from porosity to estimate saturated moisture content. Field capacity and wilting point values were extracted from the water retention properties related to soil texture listed in [35]. Following [23], the macroporosity factor, $m(3)$, was taken as 10 for the surface soil layer, 5 for the second layer, and 2 for all subsequent layers. Specific soil properties used for modeling the two watersheds are in [25].

5. Methods

5.1. Evaluating the integrated response

Two years of observed flow data, from 11/1/97 to 10/31/99, were used for comparing streamflow simulations of Town Brook, USGS stream gauge ID 01421618. Six-month periods corresponding to the wet/snow/snowmelt and dry/non-snowmelt months were investigated separately to isolate potential model accuracy problems associated with SMR's current, very simple snowmelt algorithm.

Biscuit Brook was modeled for streamflow for only 4.5 months, 5/1/99 to 9/15/99, because mechanical problems at the gauge associated with ice and other weather difficulties restricted streamflow measurements in this period, USGS stream gauge ID 01434025.

5.2. Evaluating the distributed response

The distributed response of the model was assessed by two methods: (1) comparing measured and simulated soil moisture along transects and (2) comparing simulated and Global Positioning System (GPS)-mapped wet areas, or HSA's, in a sub-basin of Town Brook.
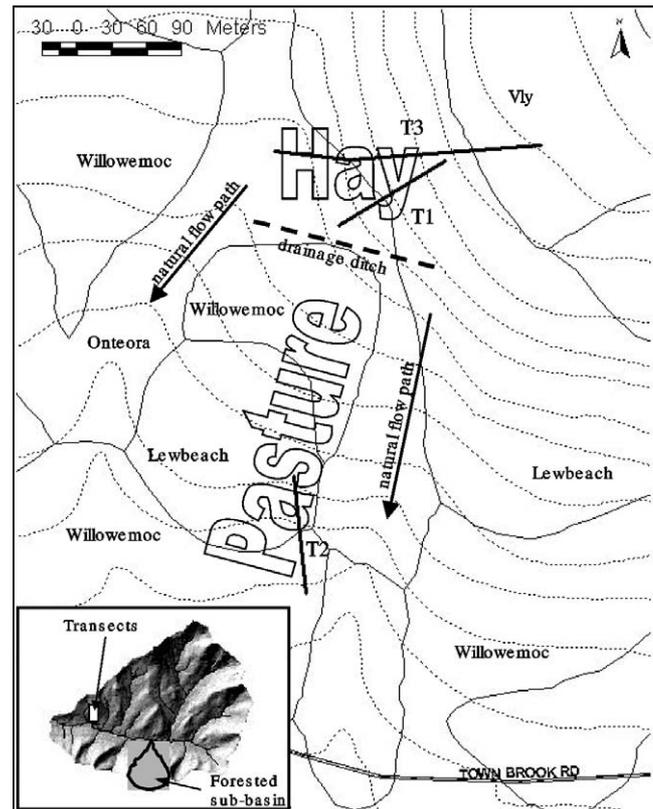

Figure 3. Location and layout of transects within the Town Brook Watershed with and location of forested sub-basin (inset). Dotted lines = USGS 20 ft contours; heavy solid lines = transects; polygons = soil types.

Soil moisture along transects. Simulated moisture contents were compared with measured soil moisture contents from three transects. Figure 3 shows the layout of the three transects: T1, T2, and T3, established on a farm in the Town Brook watershed. The transects covered 4 primary soil types and 2 different landuses. Soil samples from the 3–8 cm depth were collected at 10 m intervals along each transect and analyzed for volumetric moisture content using standard methods [39]. Transect T1, 110 m long in a hay field, was sampled on 11/3/00 after a 15 d dry period following a 1.5 cm rain event. Transect T2, 90 m long in a pasture, was sampled on 11/28/00 after a 1.3 cm cumulative rain over the previous three days. Transect T3, 230 m long on the same hayfield as T1, was sampled on 4/25/01 after 0.1 cm of rain on the previous day.

Mapping saturated areas. A 2 km^2 forested sub-basin of Town Brook (figure 3, inset) provided a unique opportunity to test the ability of SMR to simulate the spatial distribution of persistently saturated areas, or hydrologically sensitive areas (HSA) [12]. Several of these, which primarily manifested themselves as permanent flow paths and springs, were mapped using a GPS: Trimble Pathfinder Pro XL with real time differential correction. We attempted to map all identifiable flow paths and saturated areas but it was not possible for some areas because of rough terrain and dense veg-

etation. The basin was simulated for 4/1/97–4/30/01 and a map of the cumulative frequency of saturation (CFS) was generated. The CFS for any one cell is the total number of days that cell is saturated divided by the simulation period and presented as a proportion. This approach is similar to that used by [14] to compare soil wetness to the topographic index. "Simulated HSA's" were defined as any cells with a CFS greater than twice the standard deviation of all the CFS's. This is similar to the technique used by [12] to identify HSA's for water quality risk analyses. Analyses were

carried out to test the adequacy of the model by comparing the positions of simulated and mapped HSA's.

6. Results and discussion

6.1. Integrated response

Figure 4 shows the comparison of the Town Brook hydrograph for 11/1/97–10/31/99. Table 1 shows simulation statistics for Town Brook, divided into four 6-month periods
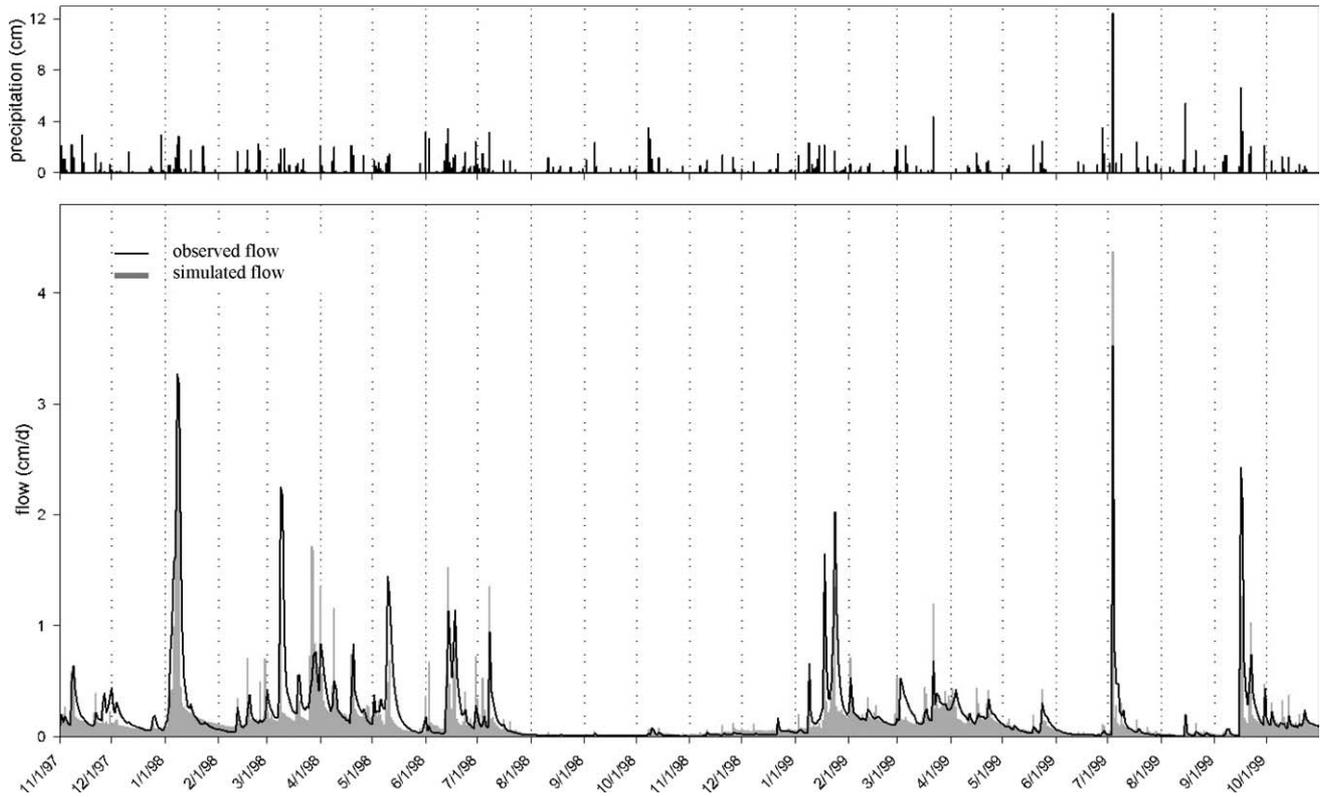

Figure 4. Town Brook simulated and observed hydrograph comparison.

Table 1
Summary of simulation statistics for Town Brook stream flow.

	Observed (cm/d)			Simulated (cm/d)			$R^{2\,a}$ (%)	$r^{2\,b}$	Ste^c (cm/d)	MCE^d (cm/d)
	mean	max	min	mean	max	min				
Winter^e '97–'98	0.32	3.27	0.039	0.28	3.02	0.037	72	0.65	0.18	–0.04
Summer^f '98	0.12	1.45	0.007	0.12	1.55	0.009	65	0.61	0.13	–0.001
Winter^e '98–'99	0.18	2.03	0.006	0.17	1.44	0.022	74	0.67	0.10	–0.02
Summer^f '99	0.13	3.53	0.004	0.12	4.38	0.015	78	0.78	0.17	–0.01
Simulation statistics for entire period							72	0.68	0.15	–0.017

[a] R^2 = Nash–Sutcliffe efficiency.
[b] r^2 = regression coefficient.
[c] Ste = standard error of estimate.
[d] MCE = mean cumulative error.
[e] Winter = November 1st to April 30th.
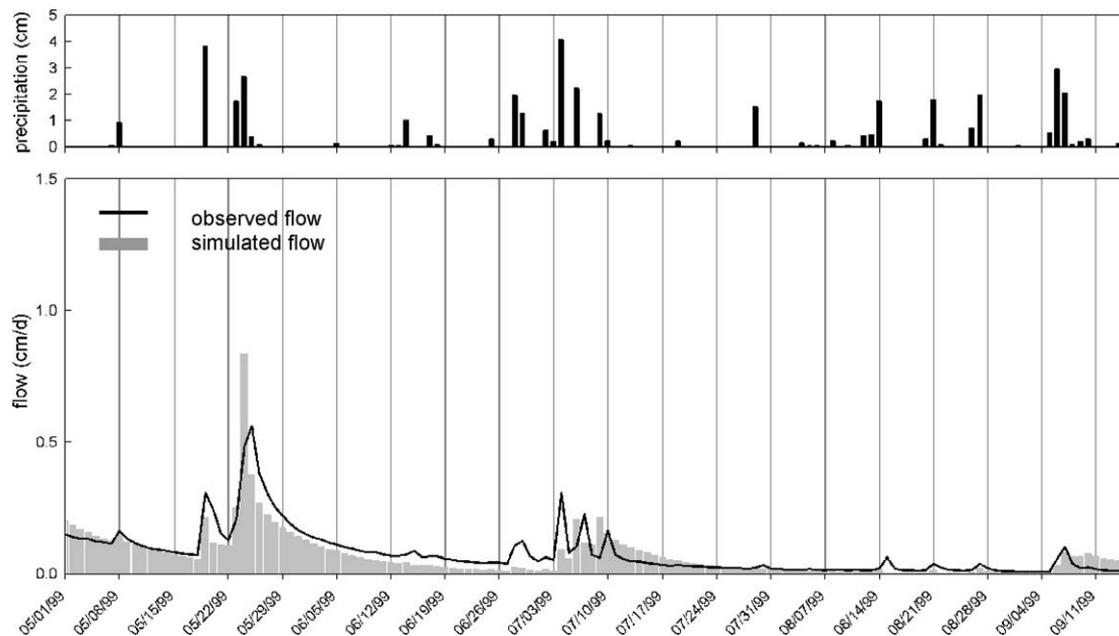[f] Summer = May 1st to October 31st.

Figure 5. Biscuit Brook simulated and observed hydrograph comparison.

to evaluate snow, i.e., winter, and non-snow, i.e. summer, periods separately. Figure 5 shows the hydrograph comparison for Biscuit Brook from 5/1/99 to 9/15/99 and table 2 summarizes the simulation statistics for Biscuit Brook. Because there is no obvious concensus among hydrologists as to the best statistics to evaluate hydrological models, we have presented multiple statistics in tables 1 and 2; all the statistics suggest similar model performance. It is often unclear what constitutes "good" model performance but, as shown in table 3, SMR compares well with other models based on published Nash–Sutcliffe, R^2, values [40].

The TOPMODEL results shown in table 3 show that TOPMODEL, like many hydrological models, required calibration because it uses parameters that are not readily measured. Because SMR uses primarily directly measured parameters it is difficult to justify model calibration. Even so, the authors briefly investigated changing some of the input parameters, especially the less certain parameters like fragipan and bedrock hydraulic conductivity, but were unable to substantially improve on the initial results. Part of SMR's success in the Catskills is attributable to earlier research that found good values for some typically unavailable hydrological, e.g., the linear groundwater reservoir coefficient [36]. Even so, it is impressive that these SMR results involved no explicit model optimization for the study watersheds and are generally comparable to the optimized, calibrated TOPMODEL results (table 3).

SMR simulated equally well in both summer and winter periods for Town Brook (table 1). This is an apparent improvement over the original SMR [10], and may be attributable to improved topographically adjusted air temperature that uses the typical dry adiabatic lapse rate to estimate the temperature as a function of elevation. The original version assumed air temperature was constant across the landscape.

The model also performed equally well for dry and wet periods. The '97–'98 winter period was wetter than the '98–'99 winter period, and the '98 summer period was wetter than the '99 summer. Table 1 shows that model evaluation statistics are constant in all periods.

Close comparison of the observed and simulated hydrographs provides insights into specific potential simulation weaknesses. There are three periods where the simulation obviously does not appear accurate, all in Town Brook – the snowmelt events following 3/9/98; the 5/10/98 event that was notably under-predicted, and the 7/4/99 event that was notably over-predicted (figure 4). Each is discussed below.

Figure 6 shows the Town Brook hydrograph for 12/28/97–4/01/98, along with temperature and precipitation inputs and simulated snowmelt/rain. The obvious over-predicted streamflow at the end of 3/98 is largely linked to the under-prediction around 3/10/98; essentially, SMR under-predicted snowmelt early in the month and, thus, had a surplus of snow that the model simulated as snowmelt later. This problem is common in many winter-time hydrology models [41]. SMR is most prone to errors when the temperature is very close to freezing or oscillating around freezing [25]. In general, the model simulated snowmelt well when a sustained period of notably above-freezing temperatures followed a period well below freezing, e.g., the substantial snowmelt event in 01/98, which was simulated reasonably well (figure 6). In addition to the perhaps overly simplified snowmelt model, temperatures used for this period were not measured within the watershed and more representative basin temperatures might improve model results with the existing snow algorithm.

The high observed peak of 5/10/98 was under-predicted notably. The cumulative precipitation recorded was 6.5 cm, whereas the cumulative observed flow during the same period was 7.9 cm (figure 4). This strongly suggests that the

Table 2
Summary of simulation statistics for Biscuit Brook stream flow.

Observed (cm/d)			Simulated (cm/d)			R^2 [a] (%)	r^2 [b]	Ste [c] (cm/d)	MCE [d] (cm/d)
mean	max	min	mean	max	min				
0.08	0.56	0.007	0.07	0.83	0.001	63	0.70	0.05	–0.009

[a] R^2 = Nash–Sutcliffe efficiency.
[b] r^2 = regression coefficient.
[c] Ste = standard error of estimate.
[d] MCE = mean cumulative error.
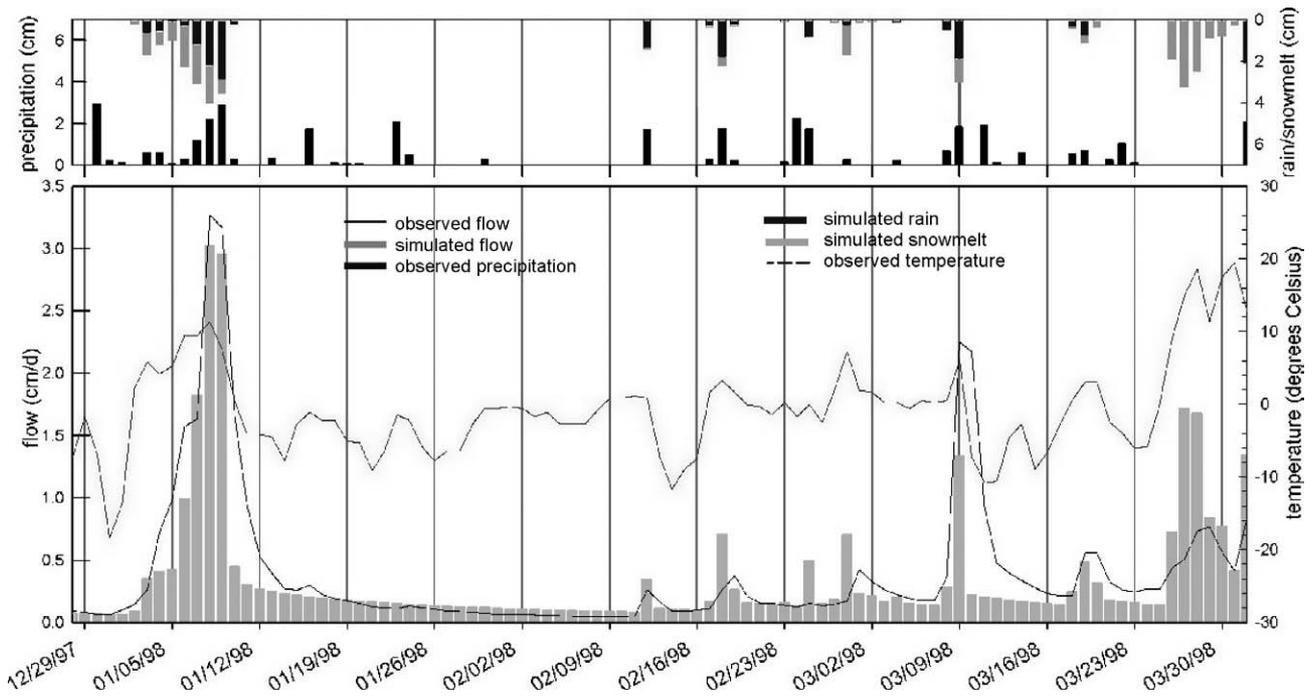
Figure 6. Town Brook hydrograph comparison showing influence of temperature on snowmelt simulation.

Table 3
Examples of Nash–Sutcliffe, R^2 for various studies.

Citations & Model	Location	R^2 (%)
SMR (this study)	Town Brook	
	Winter	72–74
	Summer	65–78
	Cumulative	72
	Biscuit Brook	63
Various modeling studies [42,43]	Durance Basin, France	
	Winter	71–83
	Summer	63–80
Various lumped, conceptual, and empirical models [44]	Various catchments and various countries	39–51
TOPMODEL [45]	Brugga catchment, Germany	
	Calibration period	85
	Post-calibration	93
TOPMODEL [46]	G1 ROOF catchment, Sweden	
	Calibration period	77
	Post-calibration	69

Figure 7. Comparison of daily precipitation from Stamford and Delhi weather stations, $r^2 = 0.23$.

actual precipitation within Town Brook on 5/10/98 may have been higher than that used as model input, i.e., the precip-

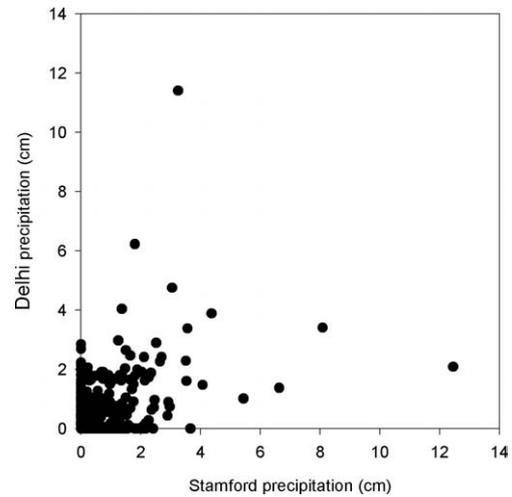itation measured at Stamford. Although unverifiable with the available data, the opposite appears to be the case for the 6/3/98 event, i.e., the input precipitation was higher than Town Brook probably received. Figure 7 is a scatter plot
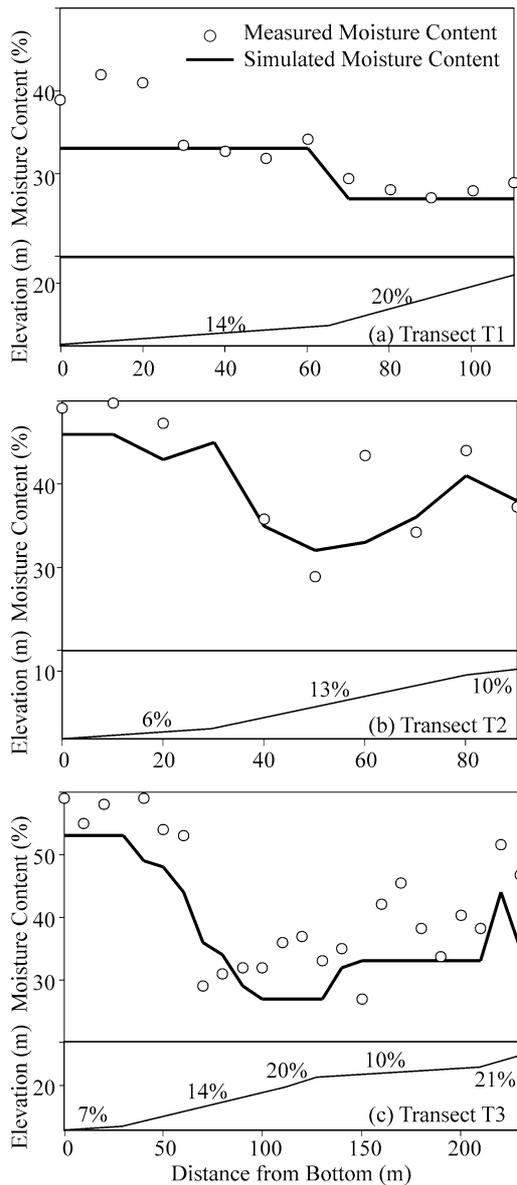
Figure 8. Simulated and measured soil moisture along transects with associated hillslope profiles.

Figure 9. Scatter plot of simulated and measured moisture contents, $r^2 = 0.79$, standard error $= 3.7\%$.

6.2. Distributed response

Although the hydrographs simulated by SMR corroborated well with measured streamflow, this does not necessarily show that the model actually captured the internal hydrological processes correctly. Models with significantly different structures can perform comparably well in simulating streamflow [19]. As discussed earlier, this study used measured soil moisture along transects and mapped saturated areas to assess SMR's ability to correctly simulate the distributed hydrology. Also, as mentioned earlier, reliable simulation of these internal processes, especially the development of saturated areas, is important to developing watershed management strategies for water quality [12].

Soil moisture along transects. Figures 8a–8c show the distributed soil moisture along transects T1–T3, respectively. Figure 9 compares predicted and observed soil moisture for all transects ($r^2 = 0.79$, Ste $= 3.7\%$) and table 4 summarizes the statistical comparisons. Simulated moisture contents show a good correlation with increasing and decreasing trends in observed soil moisture. All observed and simulated soil moistures show the expected characteristic wetting towards the low end of each transect and at breaks in the ground slope.

Transect T1 had the lowest R^2 and r^2 partially because of the low range of soil moisture during this dry period and partially because of the increase in measured soil moisture in the bottom 30 m that is not reflected in the simulated moisture (figure 8a). The observed wetness in this part of the transect, despite the prolonged dry period, is due to the redistribution of water by the artificial drainage ditch that runs at the edge of the hayfield on which transect T1 was located (figure 3). The influence of artificial diversions and ditches has not been included in this particular SMR version and, therefore, their impact was not simulated. Excluding the three obviously disparate points associated with the drainage ditch, the comparison results in $R^2 = 88\%$ for transect T1.

of two years of precipitation from Stamford and Delhi, two stations that are 30 km apart, and illustrates the high degree of spatial precipitation variability ($r^2 = 0.23$). The r^2 was 0.26 between Stamford and Walton.

The 7/4/99 event is a good example of spatially variable rainfall; 12.5, 2.0, and 0.6 cm were recorded at Stamford, Delhi, and Walton, respectively. It is not surprising, then, that this event was not one of SMR's best simulations (figure 4). The 7/4/99 storm washed out the flow gauge in Town Brook so the observed flow is itself an estimate. Also, a large storm might result in rainfall intensities high enough to generate some infiltration excess flow, which this version of SMR did not model. The considerable spatial variability of precipitation, especially in the summer months when localized thunderstorms are a common phenomenon, may explain some of the discrepancies in these periods.
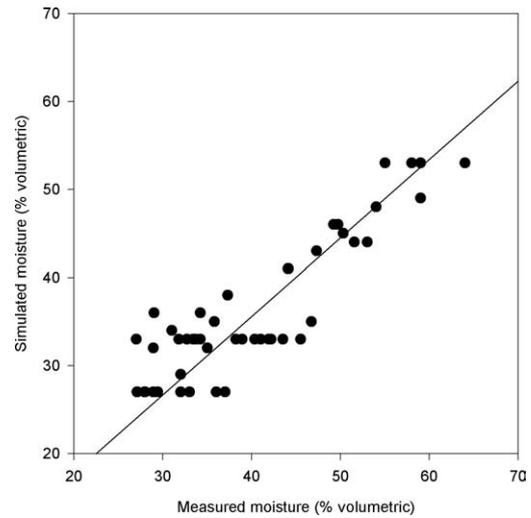
Table 4
Summary of soil moisture statistics: simulated and observed.

Transect	Observed (% volumetric)			Simulated (% volumetric)			$R^{2\,a}$ (%)	$r^{2\,b}$	Ste^c (%)
	mean	max	min	mean	max	min			
T1	33	42	27	31	33	27	35	0.63	2.0
T2	42	50	29	39	46	32	60	0.62	4.8
T3	43	64	27	38	53	27	55	0.79	4.4

[a] R^2 = Nash–Sutcliffe efficiency.
[b] r^2 = regression coefficient.
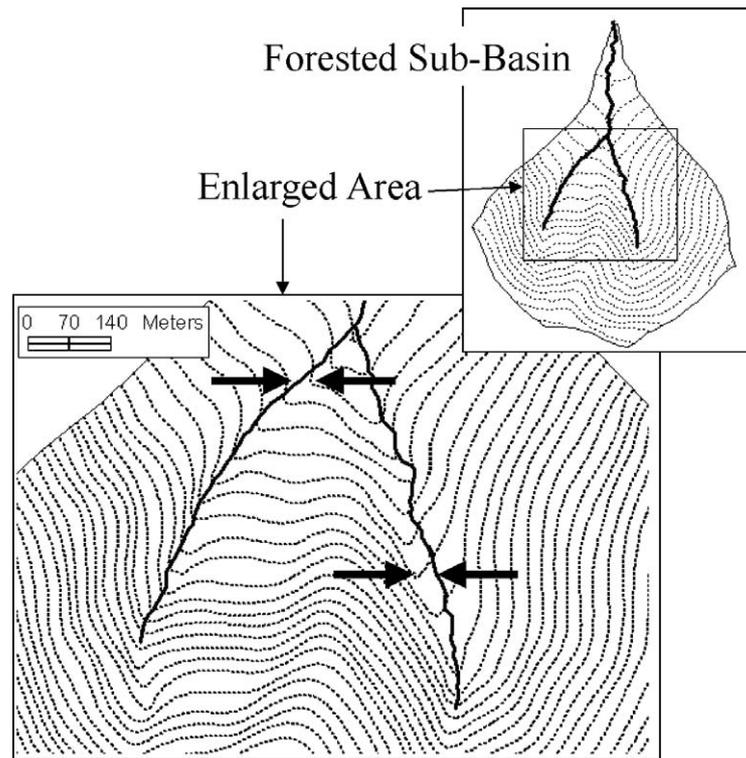[c] Ste = standard error of estimate.

Figure 11. Stream channels traced from an aerial photograph and superimposed on a DEM to show how flow path-ways are not consistently well identified by the DEM. The arrows show examples of offsets between DEM and areial photograph stream locations.

Transects T2 and T3, sampled during hydrologically active periods, show some localized variations which are not captured by SMR. Perhaps variations in the depth to the restricting layer or anomalies in the slope of the restrictive layer could explain some of the localized variations that SMR failed to produce. Also, manure was applied to transect T2's field, which affected the soil moisture in ways not addressed by SMR or most other hydrological models. The discrepancies at the down-slope end of T3, where the maximum measured moisture content was 64% (figure 8c), are due to the fact that the model was restricted by the input soil saturated moisture content of 53%. Nevertheless, SMR simulated the moisture content up to saturation, accurately reflecting the relative wetness of that part of T3.

Mapping of saturated areas.   Figure 10 shows the forested sub-basin with the GPS-mapped and simulated HSA's. Only four features, or HSA's, were obviously incorrectly simu-

lated as indicated by the arrows in figure 10. Flow paths were generally continuous and concentrated, connecting upland saturated areas to the stream channels and indicated that SMR's lack of surface routing and re-infiltration components was not of much consequence in this basin. Interestingly, a digital orthophoto aerial photograph (1 m resolution) clearly showed indications of the flow paths on the landscape that match the GPS-mapping. The digital orthophoto did not print well; however, figure 11 shows that the location of stream channels traced from a digital orthophoto do not line-up well with 10 m contours derived from the DEM. We hypothesize that the DEM may not represent microtopography well and that microtopography may control the development of some HSA's. To test this hypothesis, we manipulated the DEM by lowering the elevation at the locations where field observations and orthophoto investigations indicated rills, gullies, and other microtopographical depressions not captured by the DEM. The SMR simulation was repeated using
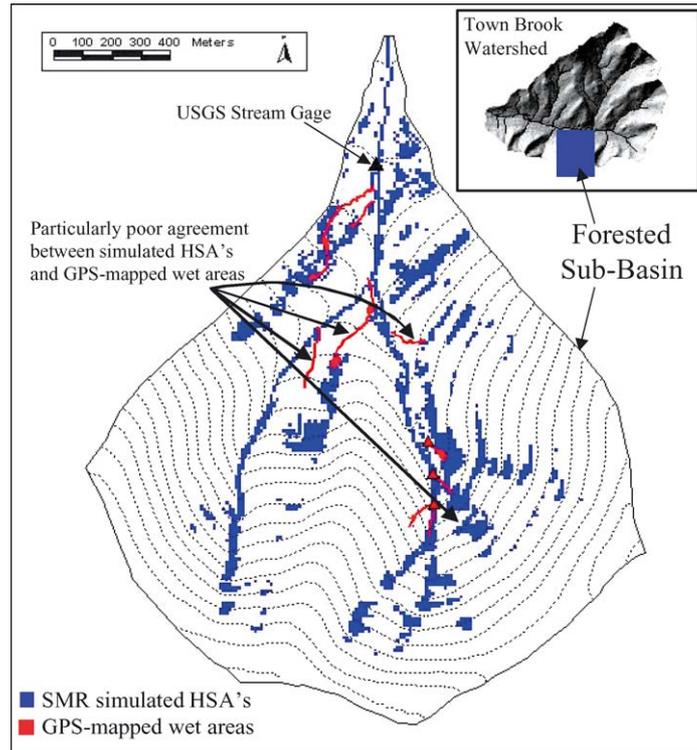
Figure 10. Mapped and simulated HSA's. The blue areas are SMR simulated HSA's and red areas are GPS mapped wet areas. The arrows indicates mapped wet areas that the model did not capture.
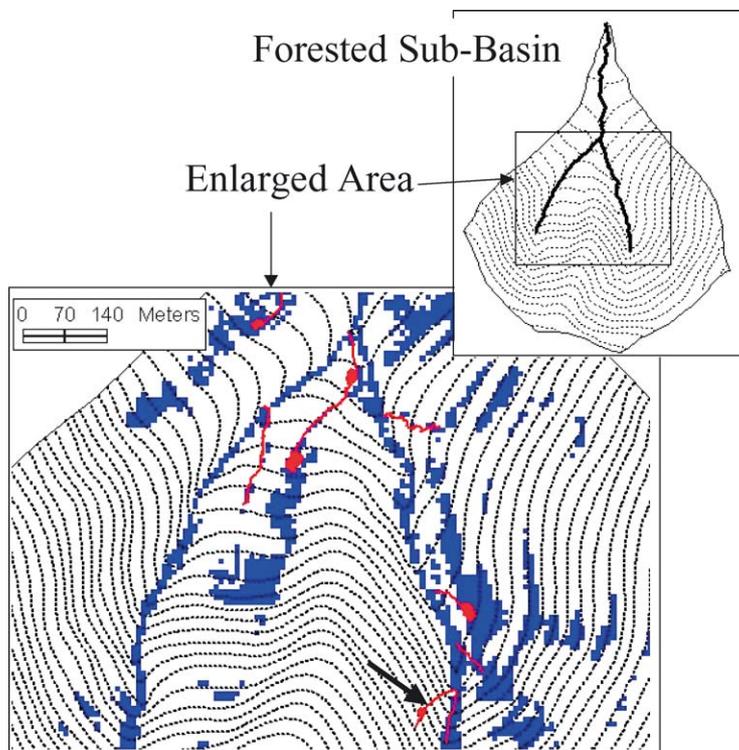

Figure 12. Mapped and simulated HSA's after correcting for microtopography. The blue areas are SMR simulated HSA's and red areas are GPS mapped wet areas. The arrow indicates a mapped wet area that the model did not capture.

the modified DEM. Figure 12 is a new map that shows a better coincidence of 3 of the 4 previously unpredicted HSA's; only the mapped area indicated by the arrow failed to produce at least some HSA along the mapped wet area. It is likely that water flow to this area is controlled by subsurface geological anomalies that are not evident from the topography (figure 12).

7. Conclusions

This study demonstrated that SMR is well-suited for modeling the hydrology of rural watersheds like Town Brook and Biscuit Brook in the NYC watershed using readily accessible data. SMR simulations showed promising corroboration with observed streamflow for both Town Brook and Biscuit Brook. Streamflow simulations were almost equally good for the wet snowmelt periods as for drier non-snowmelt periods, demonstrating an improvement over the originally published version [10]. Soil moisture simulated along transects accurately depicted the accumulation of soil moisture at toe-slopes due to the accumulation of subsurface lateral flow. Verification of the distributed response using the GPS-mapping provided new insights into SMR's ability to predict HSAs and the limitations of the input DEM.

SMR shows good potential for land management applications in rural watersheds where farmers and planners are developing strategies to reduce pollutant loadings surface waters. In particular it accurately predicted the locations of areas prone to saturation, i.e., HSA's.

Acknowledgements

References

[1] J.D. Hewlett and A.R. Hibbert, Factors affecting the response of small watersheds to precipitation in humid regions, in: *Forest Hydrology*, eds. R.C. Loeher and C.S. Martin (Pergamon Press, Oxford, England, 1967) pp. 275–290.

[2] R.E. Horton, The role of infiltration in the hydrologic cycle, Transactions of American Geophysical Union 14 (1933) 446–460.

[3] R.E. Horton, An approach toward a physical interpretation of infiltration capacity, Soil Science Society of America Proceedings 4 (1940) 399–417.

[4] M.T. Walter, V.K. Mehta, P. Gerard-Merchant, A.M. Marrone, J. Boll, T.S. Steenhuis, M.F. Walter and C.A. Scott, A simple estimation of the prevalence of Hortonian Flow in the New York City watersheds, ASCE J. Hydrol. Engrg. 8(4) (2003) 214–218.

[5] R.A. Young, C.A. Onstad, D.D. Bosch and W.P. Anderson, AGNPS: A nonpoint-source pollution model for evaluating agricultural watersheds, Journal Soil and Water Conservation 44 (1989) n2.

[6] J.G. Arnold, J.R. Williams, A.D. Nicks and N.B. Sammons, *SWRRB: A Basin Scale Formulation Model for Soil and Water Resources Management* (Texas A&M Univ. Press, College Station, TX, 1990).

[7] M.B. Abbott, J.C. Bathhurst, J.A. Cunge, P.E. O'Connell and J. Rasmussen, An introduction to the European Hydrological System – Systeme Hydrologique European, 'SHE', 1: History and philosophy of a physically-based distributed modeling system, Journal of Hydrology 87 (1986) 45–59.

[8] M.S. Wigmosta, L.W. Vail and D.P. Lettenmaier, A distributed hydrology-vegetation model for complex terrain, Water Resources Research 3 (1994) 1665–1679.

[9] V.P. Singh, Watershed modeling, in: *Computer Models of Watershed Hydrolog*, ed. V.P. Singh (Water Resources Publications, CO, 1995).

[10] J.R. Frankenberger, E.S. Brooks, M.T. Walter, M.F. Walter and T.S. Steenuis, A GIS based variable source area hydrology model, Hydrological Processes 13 (1999) 805–822.

[11] M.T. Walter and M.F. Walter, The New York City Watershed Agricultural Program (WAP): A model for comprehensive planning for water quality and agricultural economic viability, Water Resources Impact 1(5) (1999) 5–8.

[12] M.T. Walter, M.F. Walter, E.S. Brooks, T.S. Steenhuis, J. Boll and K.R. Weiler, Hydrologically sensitive areas: Variable source area hydrology implications for water quality risk assessment, Journal of Soil and Water Conservation 2 (2000) 277–284.

[13] K.J. Beven and M.J. Kirkby, A physically based variable contributing area model of basin hydrology, Hydrol. Sci. Bull. 24(1) (1979) 43–69.

[14] P.F. Quinn and K.J. Beven, Spatial and temporal predictions of soil moisture dynamics, runoff, variable source areas and evapotranspiration for Plynlimon, Mid-Wales, Hydrological Processes 7 (1993) 425–448.

[15] J.R. Frankenberger, Identification of critical runoff generating areas using a variable source area model, PhD Thesis, Dept. of Agric. and Biol. Engrg., Cornell University, Ithaca, NY (1996).

[16] R.D. Moore and J.C. Thompson, Are water table variations in a shallow forest soil consistent with the TOPMODEL concept?, Water Resources Research 32(3) (1996) 663–669.

[17] T.M. Scanlon, J.P. Raffensperger, G.M. Hornberger and R.B. Clapp, Shallow subsurface storm flow in a forested headwater catchment: Observations and modeling using a modified TOPMODEL, Water Resources Research 36(9) (2000) 2575–2586.

[18] E.S. Brooks, P.A. McDaniel and J. Boll, Hydrological modeling in watersheds of the eastern Palouse: Estimation of subsurface flow contributions, 2000 PNW-ASAE Regional Mtg, ASAE Paper 2000-10, Richland, WA (2000).

[19] M. Franchini and M. Pacciani, Comparative-analysis of several rainfall runoff models, Journal of Hydrology 122(1–4) (1991) 161–219.

[20] T.S. Steenhuis, H.K. Shimbo, W.R. Norman and D.J. Allee, Irrigation potential in the Susquehanna River Basin, Completion Report, Submitted to the Susquehanna River Basin Commission (1986).

[21] J.A. Zollweg, Effective use of geographic information systems for rainfall-runoff modeling, PhD Thesis, Dept. of Agric. and Biol. Engrg., Cornell University, Ithaca, NY (1994).

[22] J.A. Zollweg, W.J. Gburek and T.S. Steenhuis, SmoRMod – A GIS-integrated rainfall-runoff model, Trans. of the ASAE 39(4) (1996) 1299–1307.

[23] J. Boll, C.O. Stockle, S.K. Young, E.S. Brooks, J.E. Hammel, P.A. McDaniel and C.R. Campbell, Progress toward development of a GIS based water quality management tool for small rural watersheds: modification and application of a distributed model, ASAE Annu. Int. Mtg., ASAE paper 982230, Orlando, FL (1998).

[24] W.L. Kuo, T.S. Steenuis, C.E. McCulloch, C.L. Mohler, D.A. Weinstein, S.D. DeGloria and D.P. Swaney, Effect of grid size on runoff and soil moisture for a variable-source-area hydrology model, Water Resources Research 35(11) (1999) 3419–3428.

[25] V.K. Mehta, Application of a GIS-based distributed model to two Catskills watersheds, MS Thesis, Dept. of Biol. and Envir. Engrg., Cornell University, Ithaca, NY (2001).

[26] U.S. Army Corps of Engineers, Engineering and design: Runoff from snowmelt, EM 1110-2-1406, Washington, DC (1960).

[27] N. Jarvis and M. Larsson, Modeling macropore flow in soil: field validation and use for management purposes, in: *Conceptual Models of*

Flow and Transport in the Fractured Vadose Zone, eds. E.A.R. Commission on Geosciences (National Academy Press, Washington, DC, 2001) pp. 189–216.

[28] E. Bresler, D. Russo and R.D. Miller, Rapid estimate of unsaturated hydraulic conductivity function, Soil Science Society of America Proceedings 42 (1978) 170–172.

[29] T.S. Steenhuis and W.H. Van der Molen, The Thornthwaithe–Mather procedure as a simple engineering method to predict recharge, Journal of Hydrology 84 (1986) 221–229.

[30] USDA, *Soil Survey Manual*, USDA-ARS Handbook No. 18 (Washington, DC, 1993).

[31] W. Brutsaert and J.L. Nieber, Regionalized drought flow hydrographs from a mature glaciated plateau, Water Resources Research 13 (1977) 637–643.

[32] W. Brutsaert and J.P. Lopez, Basin-scale geohydrologic drought flow features of riparian aquifers in the southern Great Plains, Water Resources Research 34(2) (1998) 233–240.

[33] N.C. Brady, *The Nature and Properties of Soils* (MacMillan, NY, 1990).

[34] S.N. Asare, R.P. Rudra, W.T. Dickinson and A. Fenster, Quantification of soil macroporosity and its relationship with soil properties, Canadian Agricultural Engrg. 41(1) (1999) 23–34.

[35] D.R. Maidment, *Handbook of Hydrology* (McGraw-Hill Inc., New York, 1993).

[36] K.W. Weiler, Determination of the linear bedrock coefficient from historical data, Soil and water Lab. Tech. Rep., Dept. of Agric. and Biol. Engrg. Cornell University, Ithaca, NY (1997).

[37] J. Soren, The groundwater resources of Delaware County, New York, USGS/Water Res. Comm. Bull. GW-50, Albany, NY (1963).

[38] USDA, *Soil Survey of Ulster County, New York* (Soil Conservation Service, Washington, DC, 1975).

[39] K.A. Smith and C.E. Mullins, eds., *Soil and Environmental Analysis*, 2nd edn (Marcel Dekker, 2001) p. 637.

[40] J.E. Nash and J.V. Sutcliffe, River flow forecasting through conceptual models, I: A discussion of principles, Journal of Hydrology 10 (1970) 238–250.

[41] M.T. Walter, Winter-time hydrological modeling over a three-dimensional landscape, PhD Thesis, Biosystems Engrg. Dept., Washington State University, Pullman, WA (1995).

[42] J. Martinec and A. Rango, Merits of statistical criteria for the performance of hydrological models, Water Res. Bull. 25(2) (1989) 421–432.

[43] World Meteorological Organization (WMO), Intercomparison of snowmelt runoff, Operational hydrology Rep. no. 23, Geneva, Switzerland (1986).

[44] C. Perrin, C. Michel and V. Andreassian, Does a large number of parameters enhance model performance? Comparative assessment of common catchment model structures on 429 catchments, Journal of Hydrology 242 (2001) 275–301.

[45] A. Guntner, S. Uhlenbrook, J. Seibert and Ch. Leibundgut, Multi-criterial validation of TOPMODEL in a mountainous catchment, Hydrological Processes 13 (1999) 1603–1620.

[46] J. Seibert, K.H. Bishop and L. Nyberg, A test of TOPMODEL's ability to predict spatially distributed groundwater levels, Hydrological Processes 11 (1997) 1131–1144.